Regenerative Therapy 14 (2020) 196–204

Contents lists available at ScienceDirect

Regenerative Therapy

journal homepage: http://www.elsevier.com/locate/reth

Original Article

A cancer invasion model of cancer-associated fibroblasts aggregates combined with TGF-β1 release system

Teruki Nii [a, b], Kimiko Makino [b, c], Yasuhiko Tabata [a, *]

[a] Laboratory of Biomaterials, Institute for Frontier Life and Medical Sciences, Kyoto University, 53 Kawara-cho Shogoin, Sakyo-ku, Kyoto, 606-8507, Japan
[b] Faculty of Pharmaceutical Sciences, Tokyo University of Science, 2641, Yamazaki, Noda, 278-8510, Japan
[c] Center for Drug Delivery Research, Tokyo University of Science, 2641, Yamazaki, Noda, 278-8510, Japan

ARTICLE INFO

Article history:
Received 7 December 2019
Received in revised form
2 February 2020
Accepted 6 February 2020

Keywords:
Cancer invasion model
Anti-cancer drug screening
Three-dimensional cell culture
Drug delivery system
Gelatin hydrogel microspheres

ABSTRACT

Introduction: The objective of this study is to design a cancer invasion model where the cancer invasion rate can be regulated *in vitro*.
Methods: Cancer-associated fibroblasts (CAF) aggregates incorporating gelatin hydrogel microspheres (GM) containing various concentrations of transforming growth factor-β1 (TGF-β1) (CAF-GM-TGF-β1) were prepared. Alpha-smooth muscle actin (α-SMA) for the CAF aggregates was measured to investigate the CAF activation level by changing the concentration of TGF-β1. An invasion assay was performed to evaluate the cancer invasion rate by co-cultured of cancer cells with various CAF-GM-TGF-β1.
Results: The expression level of α-SMA for CAF increased with an increased in the TGF-β1 concentration. When co-cultured with various types of CAF-GM-TGF-β1, the cancer invasion rate was well correlated with the α-SMA level. It is conceivable that the TGF-β1 concentration could modify the level of CAF activation, leading to the invasion rate of cancer cells. In addition, at the high concentrations of TGF-β1, the effect of a matrix metalloproteinase (MMP) inhibitor on the cancer invasion rate was observed. The higher invasion rate would be achieved through the higher MMP production.
Conclusions: The present model is promising to realize the cancer invasion whose rate can be modified by changing the TGF-β1 concentration.

1. Introduction

Recently, it has being gotten harder and harder to perform animal experiments for the evaluation of biological mechanism, drug effect, and drug toxicology because of ethical issues [1,2]. For example, animal experiments for the cosmetic research and development have been prohibited since 2013 in Europe [3,4]. Based on this situation, animal-free experiments have been carried out extensively. As alternative animal models, some cell culture systems to mimic the *in vivo* environment have been developed [5–7]. Among the systems, there are many research reports on three-dimensional (3D) cell culture, such as cell aggregates, spheroids, or organoids [8–13]. In the body tissue, cells 3D interact to each other, leading to an enhanced extracellular matrix production, cytokine secretion, metabolic activity, and proliferation or differentiation [14–17]. Therefore, as one experimental trial, cell aggregates would be effective in mimicking the body system for the biological research or drug discovery [18]. However, as the size of cell aggregates become large, oxygen or nutrients supplies into the cells present in cell aggregates are too poor to survive and maintain the biological activities of cells [19,20]. In addition, it is also difficult to culture the cell aggregates for a long time period which is necessary for the *in vitro* performance of drug discovery. As one trial to tackle this issue, we have incorporated gelatin hydrogel microspheres (GM) into the cell aggregates because the oxygen and nutrients can be permeated through the water phase of GM for

Abbreviations: 2D, two-dimensional; 3D, three-dimensional; α-SMA, alpha-smooth muscle actin; CAF, cancer-associated fibroblasts; DDW, double-distilled water; ELISA, enzyme-linked immunosolvent assay; FCS, fetal calf serum; GM, gelatin hydrogel microspheres; MEM, minimum essential medium; MMP, matrix metalloproteinase; PBS, phosphate buffered-saline; PLGA, poly (lactic-*co*-glycolic acid); PVA, poly (vinyl alcohol); TGF-β1, transforming growth factor-β1.

* Corresponding author. Institute for Frontier Life and Medical Sciences, Kyoto University, 53 Kawara-cho Shogoin, Sakyo-ku, Kyoto, 606-8507, Japan. Fax: +81 75 751 4646.
E-mail address: yasuhiko@infront.kyoto-u.ac.jp (Y. Tabata).

Peer review under responsibility of the Japanese Society for Regenerative Medicine.

https://doi.org/10.1016/j.reth.2020.02.003

their supply to cells [21]. Moreover, it has been demonstrated that the GM can controlled release growth factors (e.g. basic fibroblast growth factor, transforming growth factor-β (TGF-β), or platelet-derived growth factor) or drugs (e.g. a p53 inhibitor), which is effective in enhancing the cell viability and functions [22–31]. Based on these findings, it is experimentally confirmed that cell aggregates incorporating GM containing the growth factors or drugs are promising in drug screening or regenerative medicine [11,31–36].

Cancer invasion is one of the problems to be solved in cancer therapy because the cancer invasion leads to cancer metastasis, which often causes finally poor mortality rates [37]. Recently, it has been demonstrated that cancer cells do not have a great ability in itself to promote the invasion and that stromal cells support their invasion [31,38–40]. Among the stromal cells, cancer-associated fibroblasts (CAF) play major roles to promote the cancer invasion through the interaction with cancer cells [41]. It is reported that the cancer invasion rate by co-cultured or existence with CAF is significantly higher than that of CAF-free culture *in vitro* or *in vivo* [42–47]. Although several factors are secreted by the interaction, matrix metalloproteinase (MMP) is essential for the cancer invasion because MMP has an ability to degrade the basement membrane [41,48,49]. Based on the findings, it has been noted that the cancer invasion therapy to target CAF or the research of interaction between cancer cells and CAF would be effective [31,41,50–53]. In addition, growth factors also have an important influence in promoting the cancer invasion while they are physiologically secreted from several cells of cancer cells, CAF, and endothelial cells. The previous study has revealed that CAF stimulated by TGF-β1 increase the cancer invasion rate in a population study [54]. TGF-β1 is one of the important growth factors for interaction between cancer cells and CAF via MMP, leading to the cancer invasion as shown in Fig. 1 [54–56]. The objective of this study is to design a cancer invasion model where the cancer invasion rate can be regulating by changing the concentration of TGF-β1. To replicate the cancer invasion via CAF activation by TGF-β1, first, we prepared CAF aggregates incorporating GM capable of TGF-β1 controlled release. Then, alpha-smooth muscle actin (α-SMA) for the CAF aggregates was measured to investigate the CAF activation level by changing the concentration of TGF-β1. An invasion assay was performed to evaluate the cancer invasion rate by co-cultured of cancer cells with various CAF aggregates incorporating GM containing TGF-β1. We examined the effect of a MMP inhibition treatment on the secretion level of MMP and the cancer invasion rate.

2. Materials and methods

2.1. Preparation of GM

Gelatin hydrogel microspheres (GM) were prepared by the chemical crosslinking of gelatin in a water-in-oil emulsion state according to the method previously reported [25]. Briefly, an aqueous solution (20 ml) of 10 wt % gelatin (isoelectric point 5.0, weight-averaged molecular weight = 100,000, Nitta Gelatin Inc., Osaka, Japan) was preheated at 40 °elatin hydrogel microspheres (GM) were prepared by the chemical crosslinking of gelatin in a water-in-oil emulsion state according to the method previously reported [25]. Briefly, an aqueous solution (20 ml) of 10 wt % gelatin (isoeleting GM were washed three times with cold acetone in combination with centrifugation (5000 rpm, 4 °C, 5 min) to completely exclude the residual oil. Then, GM were fractionated by size using sieves with apertures of 32 and 53 μm (Iida Seisakusho Ltd, Osaka, Japan) and air dried at 4 °C. Then, non-crosslinked and dried GM (200 mg) were treated in a vacuum oven at 140 °elatin hydrogel microspheres (GM) were prepared by the chemical crosslinking of gelatin in a water-in-oil emulsion state according to the methOsaka, Japan). The size of 100 microspheres for each sample was measured using the computer program Image J (NIH Inc., Bethesda, USA) to calculate the average diameters.

2.2. Preparation of GM-TGF-β1

Recombinant human TGF-β1 (R&D Systems, Inc., Minneapolis, USA) was dissolved in double-distilled water (DDW) to give a solution at TGF-β1 concentration of 10, 100, 500, 1000, and 5000 μg/ml. The TGF-β1 solution (20 μl) was dropped into 2 mg of freeze-dried GM, followed by leaving at 37 °C overnight for the impregnation of TGF-β1 into the GM to prepare GM containing TGF-β1 (GM-TGF-β1). GM-TGF-β1 containing 10, 100, 500, 1000, and 5000 μg/ml TGF-β1 were named GM-10TGF-β1, GM-100TGF-β1,

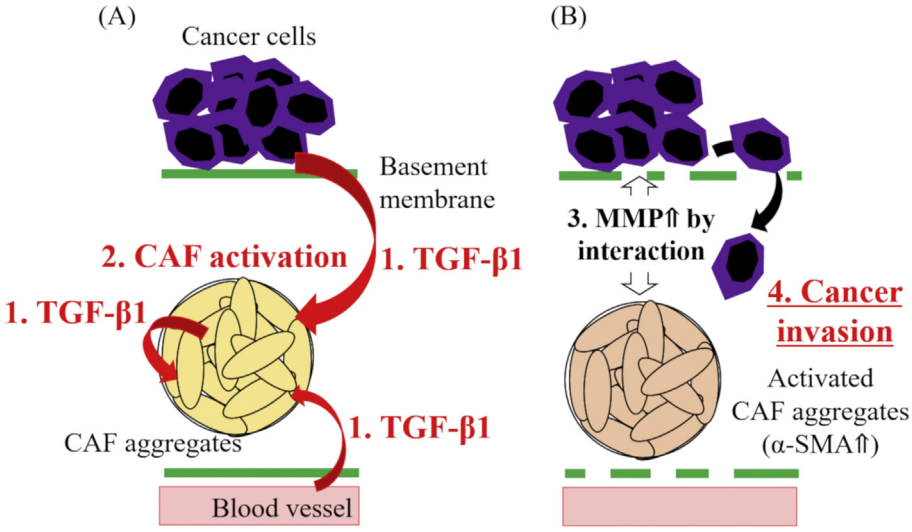

Fig. 1. Characterization of cancer invasion by the cell culture system of interaction between cancer cells and CAF (A) TGF-β1 secreted from cancer cells, endothelial cells or CAF aggregates is able to stimulate or activate CAF aggregates (A higher α-SMA expression level for CAF) (B) Cancer cells and activated CAF sustainably interact to each other, leading to an accelerated MMP production. MMP could degrade the basement membrane, resulting in an enhanced cancer invasion.

GM-500TGF-β1, GM-1000TGF-β1, and GM-5000TGF-β1, respectively. The TGF-β1 solution was completely absorbed into the GM through the impregnation process because the solution volume was much less than theoretically required for the equilibrated swelling of GM.

2.3. Evaluation of in vitro TGF-β1 release

GM-5000TGF-β1 (2 mg) were incubated in 9.57 mM phosphate-buffered saline solution (PBS, pH 7.4). At each point, the buffer was removed and replaced with fresh PBS. After 24 hr, PBS was replaced with collagenase. TGF-β1 concentrations released from GM were measured using human TGF-β1 ELISA kit (Proteintech Inc., Rosemont, USA).

2.4. Cell culture experiments

WA-hT cells of human small cell carcinoma cell line (RIKEN, Japan) and WA-mFib cells of cancer-associated fibroblasts (CAF) cell line derived WA-hT were cultured in minimum essential medium (MEM) (Sigma–Aldrich Co. LLC. St. Louis, USA) supplemented with 10 vol % fetal calf serum (FCS) (Thermo Inc. Waltham, USA), penicillin (50 U/mL), and streptomycin (50 U/mL) (standard medium) and cultured at 37 °A-hT cells of human small cell carcinoma cell lin.

2.5. Preparation of various CAF aggregates

A Poly (vinyl alcohol) (PVA) sample (the degree of polymerization = 1800 and the saponification = 88 mol %) kindly supplied from Unichika (Tokyo, Japan) was dissolved in PBS (1 wt %). The PVA solution was added to each well of round-bottomed (U-bottomed) 96-well culture plate (200 μl/well) and incubated at 37° Poly (vinyl alcohol) (PVA) sample (tremoved by aspiration and the wells washed twice with PBS (200 μl/well). GM, various GM-TGF-β1, and CAF suspensions were separately suspended in the standard medium. After the suspensions of GM (2×10^3 microspheres/ml, 100 μl) and various GM-TGF-β1 (2×10^3 microspheres/ml, 100 μl) were prepared, CAF suspensions (2.0×10^4 cells/ml, 100 μl) were mixed. The mixtures were added to the wells coated. As a control group, CAF aggregates incorporating GM by addition of free TGF-β1 solution (5000 μg/ml) into the culture medium were cultured. The addition schedule is followed: 20% of TGF-β1 amount contained in GM was added when the culture was started. After 7 days, 20% of TGF-β1 amount was added on day 7, 8, 9, and 10 for 4 days (Fig. 2B). In addition, the CAF aggregates were not cultured 10 days later because the amount of TGF-β1 added into the culture medium was higher than that of TGF-β1 contained in GM. The pictures of the various types of CAF aggregates were taken with a microscope (CKX41, Olympus Ltd, Tokyo, Japan). The size of CAF aggregates was measured using the computer program Image J (NIH Inc., Bethesda, USA) to calculate the average diameter. CAF aggregates incorporating GM, GM-10TGF-β1, GM-100TGF-β1, GM-500TGF-β1, GM-1000TGF-β1, and GM-5000TGF-β1 were named CAF-GM, CAF-GM-10TGF-β1, CAF-GM-100TGF-β1, CAF-GM-500TGF-β1, CAF-GM-1000TGF-β1, and CAF-GM-5000TGF-β1, respectively (Fig. 2A). In addition, CAF-GM by addition of free TGF-β1 solution was named CAF-GM + fTGF-β1.

2.6. Evaluation of cell number

To evaluate the cell number in CAF-GM, various CAF-GM-TGF-β1, and CAF-GM + fTGF-β1, CAF aggregates were taken into a microtube. After their centrifugation, the culture medium was carefully removed and the CAF aggregates were washed with 200 μl of PBS. After removing PBS, 200 μl of collagenase was added and samples were incubated at 37 °C for 30 min to allow to completely degrade GM. Then, 50 μl of 2.5 g/l-trypsin and 1 mmol/l-EDTA solution (Nacali tesque, Inc., Kyoto, Japan) was added and samples were incubated at 37 °C for 30 min while they were pipetted every 5 min to facilitate the dissociation of CAF aggregates. The enzyme

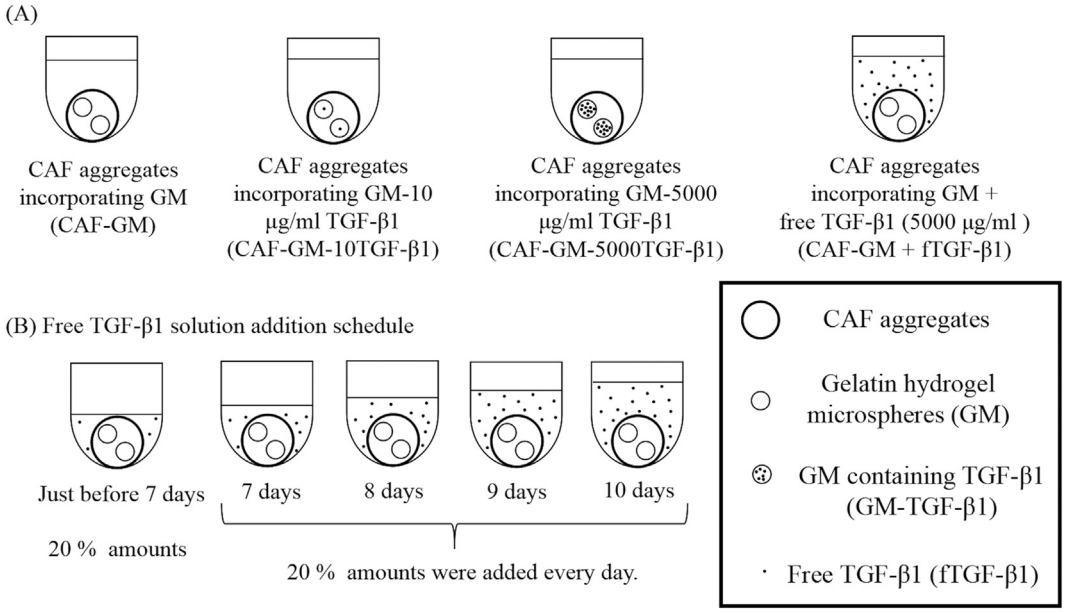

Fig. 2. (A) Preparation of CAF aggregates incorporating GM (CAF-GM), CAF aggregates incorporating GM containing various concentrations (10, 100, 500, 1000, and 5000 μg/ml) of TGF-β1 (CAF-GM-10TGF-β1, CAF-GM-100TGF-β1, CAF-GM-500TGF-β1, CAF-GM-1000TGF-β1, and CAF-GM-5000TGF-β1), and CAF aggregates incorporating GM in the presence of free TGF-β1 (CAF-GM + fTGF-β1) (B) Time schedule of free TGF-β1 solution addition in the culture medium. When the culture was started, 20% of total TGF-β1 amounts was added. After 7 days after incubation, 20% of total amounts was added on day 7, 8, 9, and 10. The total amount of TGF-β1 added was the same as that of TGF-β1 incorporated 10 days after incubation.

action was stopped by the addition of 50 μl of culture medium. The total cell number per cell aggregates was measured.

2.7. Evaluation of α-SMA expression level

To evaluate the level of alpha-smooth muscle actin (α-SMA) expression, various types of CAF aggregates were measured by using alpha-smooth muscle actin ELISA kit (NBP2-66429) (Novus Biologicals, LLC, New York, USA). The α-SMA expression level was calculated by dividing the total cell number.

2.8. Invasion assay

To evaluate the cancer invasion ability by co-culture of cancer cells with various types of CAF aggregates, the cancer invasion assay was performed by using Cytoselect 96 well invasion assay (Cell Biolabs, Inc., San Diego, USA). In brief, 150 μl of CAF aggregates (10 days after incubation) was added (150 μl) into the tubes. The tubes were centrifuged and the supernatant was removed. Then, 800 μg/ml of an MMP inhibitor or standard medium was added (150 μl) to the tubes, and the suspensions were plated to the well of feeder tray. After the membrane chamber was placed into the feeder tray, the cancer cell suspension (100 μl, 2.0×10^5 cells/well in FCS-free medium) was added to the membrane chamber. The samples were incubated for 24 hr. After completely dislodging the cancer cells from the underside of the membrane, the lysis buffer dye solution was added. Then, the fluorescent intensity was measured in a fluorescence spectrometer (F-2000, HITACHI Ltd, Tokyo, Japan) at excitation and emission wavelengths of 480 and 520 nm, respectively. Calculation of cancer invasion rate was followed:

$$\text{Invasion rate} = \frac{\textit{Cell number of cancer cells in underside of the membrane}}{2.0 \times 10^5 \text{ cells}} \times 100$$

Moreover, the culture medium was collected, and then the amount of MMP-2 secreted was measured by total MMP-2 quantikine ELISA kit (MMP200) (R&D Systems, Inc., Minneapolis, USA).

2.9. Statistical analysis

All the data were statistically analyzed and expressed as the mean ± the standard error of the mean. The data were analyzed by student t-test or Tukey's test to determine the statistically significant difference while the significance was accepted at $p < 0.05$. Experiments for each sample were performed three wells independently unless otherwise mentioned.

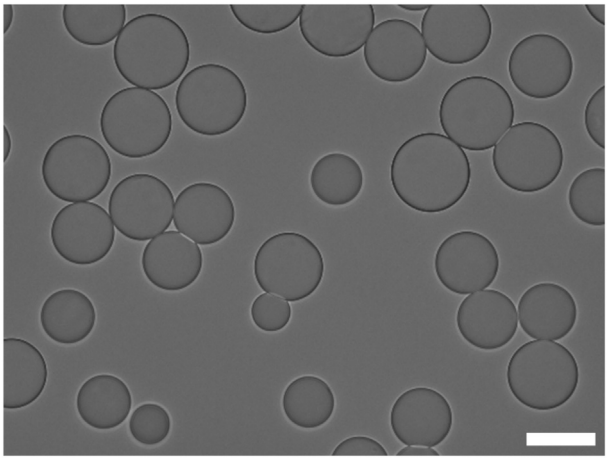

Fig. 3. A light microscope photograph of GM dispersed in the water. Scale bar; 50 μm.

3. Results

3.1. Morphology of GM

Fig. 3 shows the microscope picture of GM. The GM were spherical and had a smooth surface. The size in the swollen condition ranged 46.5 ± 5.18 μm.

3.2. Time profile of TGF-β1 release from GM-TGF-β1

Fig. 4 shows the TGF-β1 release profile from GM-TGF-5000β1. When GM-5000TGF-β1 were incubated into PBS, an initial slow release of TGF-β1 was observed. On the other hand, TGF-β1 was released with time by the addition of collagenase.

3.3. Characterization of CAF-GM, CAF-GM-TGF-β1, and CAF-GM + fTGF-β1

Fig. 5 shows the light microscope pictures of CAF-GM, CAF-GM-TGF-β1, and CAF-GM + fTGF-β1. All types of CAF aggregates were formed 7 days after incubation. The TGF-β1 presence, the TGF-β1 concentrations, and the addition of free TGF-β1 solution did not affect the morphology or size of aggregates (Figs. 5 and 6). In addition, the size of CAF aggregates 15 days after incubation was significantly smaller than that 10 days later.

3.4. Cell number in CAF-GM, various types of CAF-GM-TGF-β1, and CAF-GM + fTGF-β1

Fig. 7 shows the cell number for CAF-GM, CAF-GM-TGF-β1, and CAF-GM + fTGF-β1. TGF-β1 presence, the TGF-β1 concentrations, and the addition of free TGF-β1 solution did not affect the cell number. In addition, the cell number 10 days after incubation was significantly higher than that 5 days later.

3.5. α-SMA expression level of CAF-GM, various types of CAF-GM-TGF-β1, and CAF-GM + fTGF-β1

To evaluate the effect of TGF-β1 on the CAF activation, α-SMA expression level was measured 5, 10, and 15 days after incubation (Fig. 8). There was no significantly different in the α-SMA

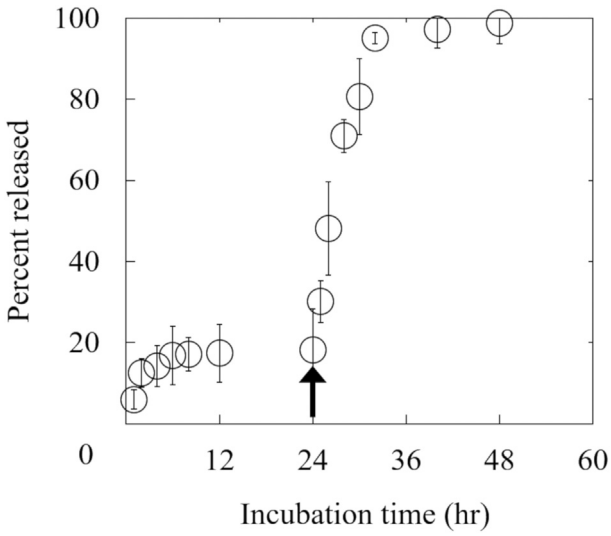

Fig. 4. *In vitro* time profile of TGF-β1 from GM-5000TGF-β1. Collagenase was added into PBS at 24 hr indicated by the arrow.

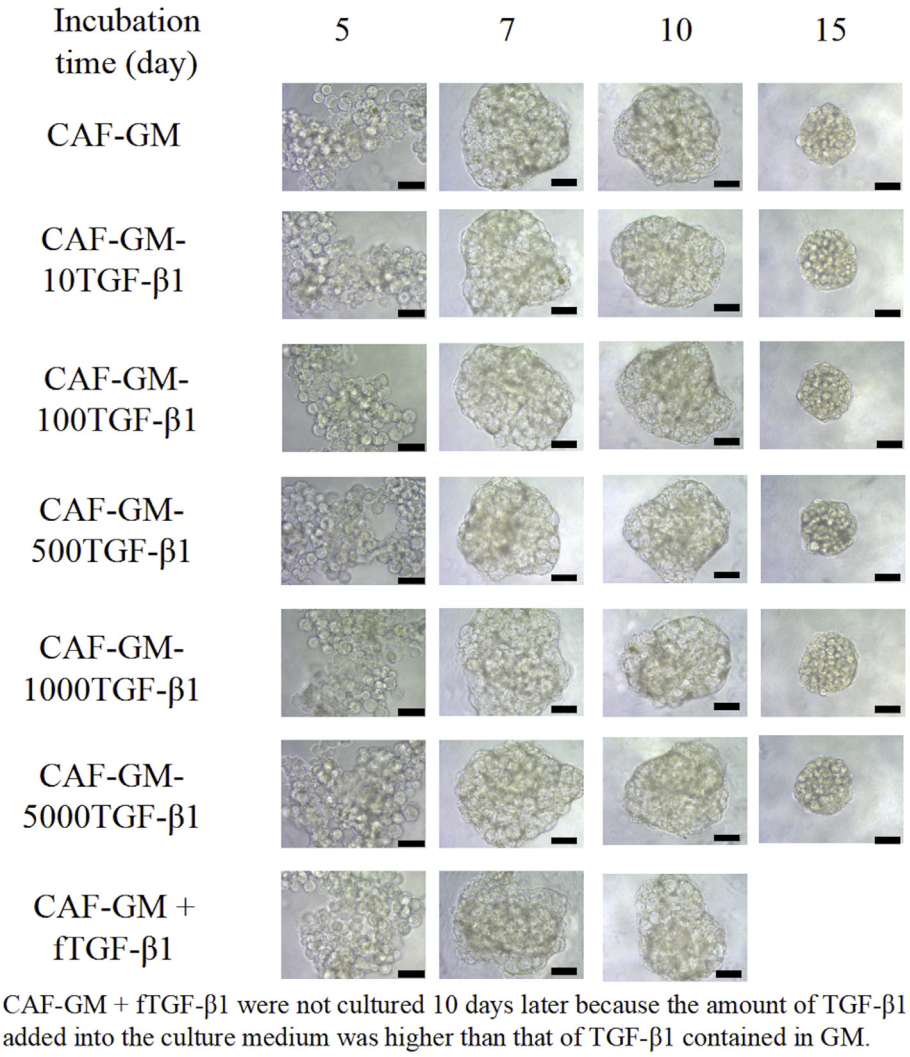

Fig. 5. Light microscope photographs of CAF-GM, CAF-GM-10TGF-β1, CAF-GM-100TGF-β1, CAF-GM-500TGF-β1, CAF-GM-1000TGF-β1, and CAF-GM-5000TGF-β1 5, 7, 10, and 15 days after incubation or that of CAF-GM + fTGF-β1 5, 7, and 10 days after incubation. Scale bar; 200 μm.

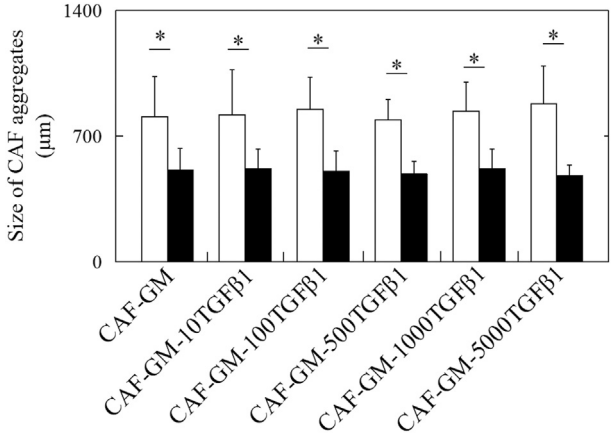

Fig. 6. Size of CAF aggregates for CAF-GM, CAF-GM-10TGF-β1, CAF-GM-100TGF-β1, CAF-GM-500TGF-β1, CAF-GM-1000TGF-β1, and CAF-GM-5000TGF-β1 groups 10 (□), and 15 days after incubation (■). *$p < 0.05$; significantly difference between the two groups.

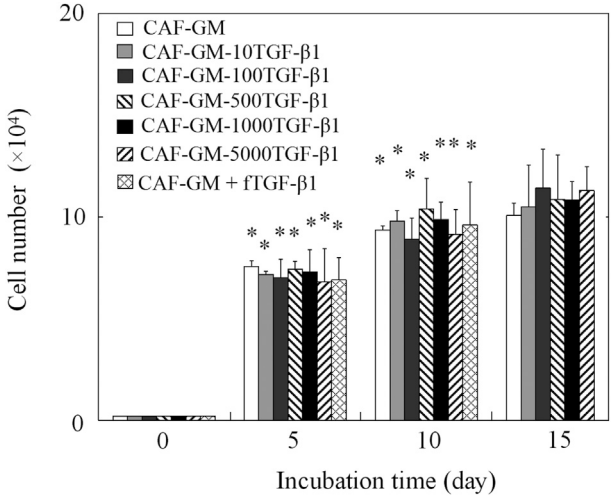

Fig. 7. Cell number of CAF aggregates for CAF-GM, CAF-GM-10TGF-β1, CAF-GM-100TGF-β1, CAF-GM-500TGF-β1, CAF-GM-1000TGF-β1, and CAF-GM-5000TGF-β1 groups 5, 10, and 15 days after incubation or CAF-GM + fTGF-β1 5 and 10 days after incubation. *$p < 0.05$; significantly difference against the cell number for the same condition of CAF 5 days before.

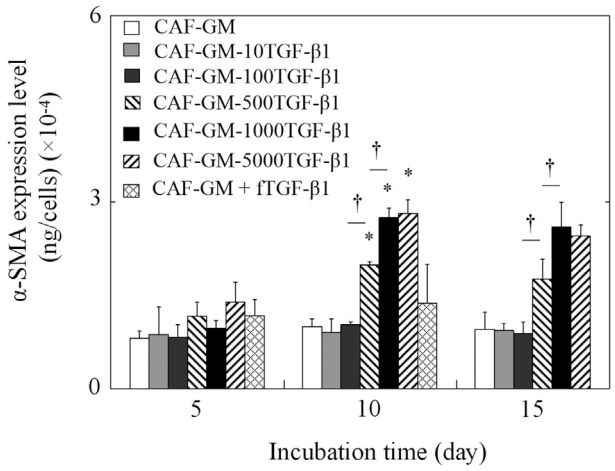

Fig. 8. α-SMA expression level of CAF aggregates for CAF-GM, CAF-GM-10TGF-β1, CAF-GM-100TGF-β1, CAF-GM-500TGF-β1, CAF-GM-1000TGF-β1, and CAF-GM-5000TGF-β1 groups 5, 10, and 15 days after incubation or CAF-GM + fTGF-β1 5 and 10 days after incubation. *$p < 0.05$; significantly difference against the α-SMA expression level for the same condition of CAF 5 days before. †$p < 0.05$; significantly difference between the two groups.

expression level among all types of CAF 5 days after incubation. However, 10 and 15 days after incubation, the α-SMA expression level for CAF-GM-500TGF-β1 was significantly higher than that for CAF-GM, CAF-GM-10TGF-β1, and CAF-GM-100TGF-β1. Although the α-SMA expression level for CAF-GM-1000TGF-β1 was significantly higher than that for CAF-GM-500TGF-β1, there was no significance difference between the CAF-GM-1000TGF-β1 and CAF-GM-5000TGF-β1. In addition, the α-SMA expression level for CAF-GM + fTGF-β1 was not significantly different from that for CAF-GM, CAF-GM-10TGF-β1, or CAF-GM-100TGF-β1 5 and 10 days after incubation.

3.6. Invasion assay

Fig. 9A shows that the invasion rate of cancer cells by co-cultured with CAF-GM, various CAF-GM-TGF-β1, and CAF-GM + fTGF-β1. Fig. 9B shows that the correlation between the invasion rate and α-SMA expression level. The coefficient of determination was about 0.87. In addition, Fig. 9C shows that the correlation between the invasion rate and the TGF-β1 concentration. The coefficient of determination was about 0.96. Fig. 10 shows that the invasion rate of cancer cells by MMP inhibitor. The invasion rate of cancer cells by co-cultured with CAF-GM-500TGF-β1, CAF-GM-1000TGF-β1, and CAF-GM-5000TGF-β1 decreased by MMP inhibitor. However, the effect of MMP inhibitor was not observed in CAF-GM, CAF-GM-10TGF-β1, CAF-GM-100TGF-β1, and CAF-GM + fTGF-β1. Moreover, secretion level of MMP-2 had an important role in cancer invasion rate (Fig. 11).

4. Discussion

For the combination with cell aggregates, various microspheres of gelatin [11,57,58], poly (lactic-*co*-glycolic acid) (PLGA) [59–62], and alginate [63,64] were investigated. Among these materials, in this study, gelatin was used because of the high cell adhesiveness or lower cytotoxicity [65–67]. GM used in this study were of

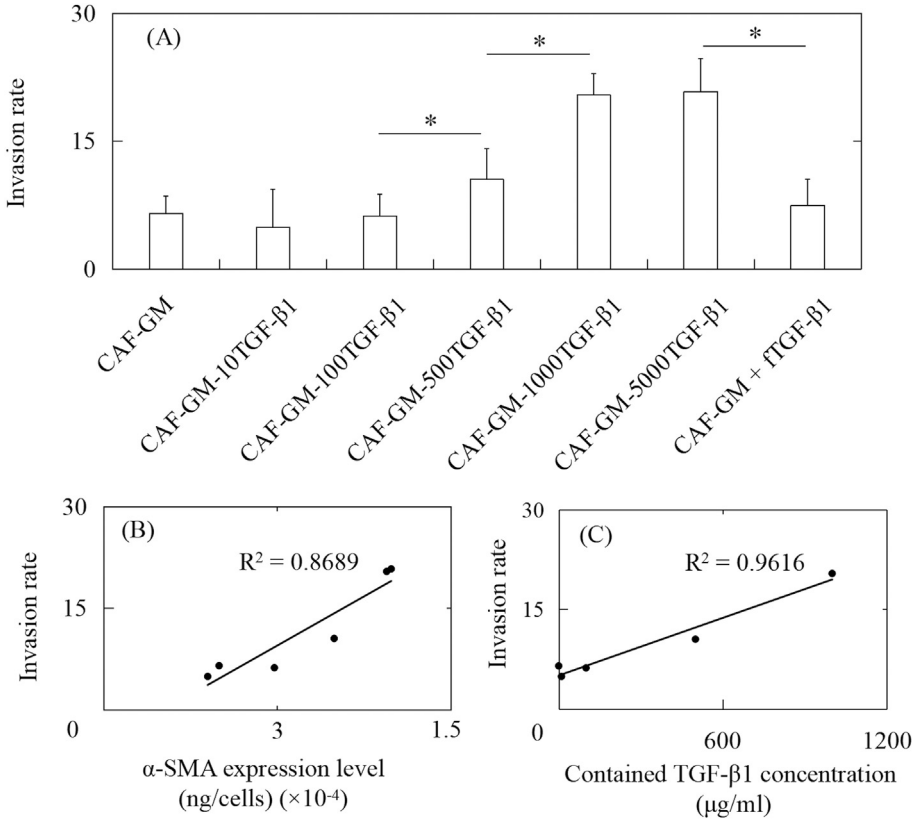

Fig. 9. (A) Invasion rate of cancer cells by co-cultured with CAF-GM, CAF-GM-10TGF-β1, CAF-GM-100TGF-β1, CAF-GM-500TGF-β1, CAF-GM-1000TGF-β1, CAF-GM-5000TGF-β1, and CAF-GM + fTGF-β1 groups 1 days after incubation. *$p < 0.05$; significantly difference between the two groups (B) Correlation between the α-SMA expression level and the invasion rate (C) Correlation between the TGF-β1 concentration and the invasion rate.

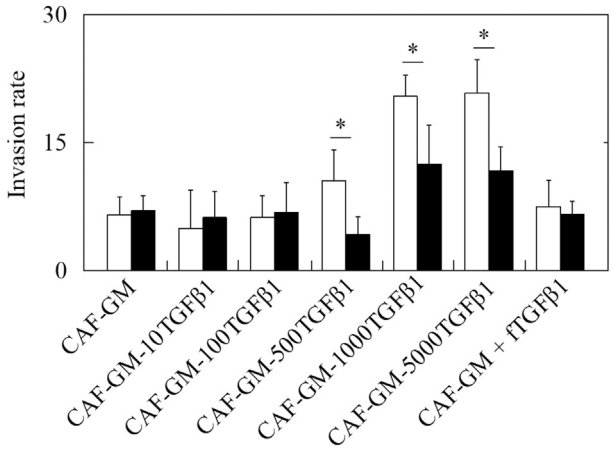

Fig. 10. Invasion rate of cancer cells by co-cultured with CAF-GM, CAF-GM-10TGF-β1, CAF-GM-100TGF-β1, CAF-GM-500TGF-β1, CAF-GM-1000TGF-β1, CAF-GM-5000TGF-β1 groups, and CAF-GM + fTGF-β1 1 days after incubation: culture without (□) or with MMP inhibitor addition (■). *$p < 0.05$; significantly difference between the two groups.

32–53 μm in diameter dehydrothermally crosslinked for 72 hr. Because our previous study demonstrates that GM with this property is good for the purpose of cell aggregates incorporating GM [68]. In terms of the mixing ratio of cells to GM, 10:1 was selected because this mixing ratio was appropriate to form the cell aggregates incorporating GM [11]. In addition, in this study, two-dimensional CAF and CAF aggregates without GM were not prepared as controls. Because the biological functions of 2D CAF and CAF aggregates without GM were found to be much lower than that of CAF-GM due to the lower cell–cell contact and rapid cell death, respectively [31].

In our previous study, proliferation of bone marrow stem cells was improved based on the TGF-β1 controlled release from GM-TGF-β1 [28]. TGF-β1 slow release from GM-TGF-β1 can enhance cell activity or functions. However, the effect of the TGF-β1 controlled release from GM-TGF-β1 on the CAF functions has not been studied. From the TGF-β1 release profile, about 20% of TGF-β1 total amount was initially released from GM-TGF-β1 in PBS. Our previous studies revealed that TGF-β1 could be controlled release from GM [28]. By the addition of collagenase, TGF-β1 was released with time. It is likely that TGF-β1 was released as the gelatin degradation of GM by collagenase. In addition, the TGF-β1 concentration did not affect the drug release profile (data not shown). The number of gelatin molecules would be large enough to molecularly associate with TGF-β1.

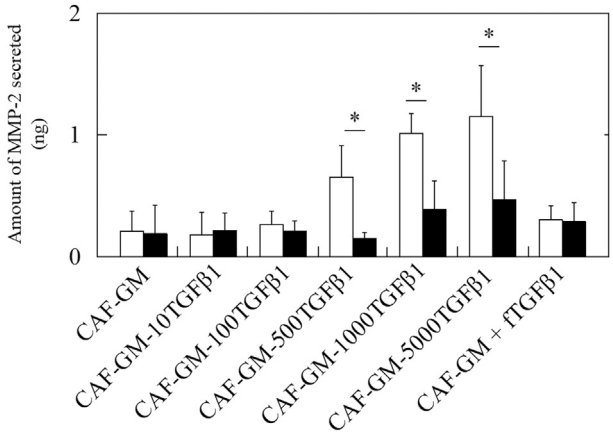

Fig. 11. Amount of MMP-2 secreted by co-cultured with CAF-GM, CAF-GM-10TGF-β1, CAF-GM-100TGF-β1, CAF-GM-500TGF-β1, CAF-GM-1000TGF-β1, CAF-GM-5000TGF-β1, and CAF-GM + fTGF-β1 groups 1 days after incubation: culture without (□) and with MMP inhibitor addition (■). *$p < 0.05$; significantly difference between the two groups.

To claim the advantageous effect of TGF-β1 release "inside" CAF aggregates, free TGF-β1 solution was daily added into the CAF-GM culture medium. To this end, it is important to determine the addition schedule considering the release profile. From Fig. 4 and 20% of total TGF-β1 amount contained was initially released in PBS, followed by the controlled TGF-β1 release as the result of GM degradation with time was observed. Based on the release profile, at the starting point of culture, 20% of total TGF-β1 amount was added into the culture medium. After CAF-GM were formed (7 days), 20% of total TGF-β1 amount was added every day (Fig. 2B). It has been reported that cell aggregates produce the enzyme, cytokine, or chemokine much more efficiently than non-aggregated cells [15,16,18]. At 10 days, the amount of free TGF-β1 solution is the same as that of TGF-β1 contained. We can say with certainty that the total amount of TGF-β1 solution is not lower than that of TGF-β1 released from GM-TGF-β1. Taken together, we could evaluate the effect of TGF-β1 released in CAF aggregates 10 days after incubation. It is no doubt that the time schedule of TGF-β1 addition does not always simulate that of TGF-β1 released from GM-TGF-β1.

It is apparent from Figs. 5–7, the TGF-β1 present, TGF-β1 concentrations, and the addition of free TGF-β1 solution did not affect the morphology, size, and cell number. Although the reason is not clear at present, our previous study suggests that the characterization of GM did not affect these parameters [11,68]. The size of CAF aggregates 15 days after incubation was smaller than that 10 days because of the GM degradation (Figs. 5 and 6). Our previous study demonstrates that the GM degradation led to a decrease in the size of cell aggregates and biological functions of cell aggregates [11]. Based on the reasons, in this study, CAF aggregates were cultured until 15 days.

α-SMA is one of the most important markers for CAF. When the α-SMA level of CAF is high, it is experimentally characterized as CAF activation [41,69,70]. The α-SMA expression level 5 days after incubation was not significantly different. However, 10 and 15 days after incubation, the α-SMA expression level of CAF-GM-500TGF-β1 was significantly different from that of CAF-GM, CAF-GM-10TGF-β1, and CAF-GM-100TGF-β1 (Fig. 8). In addition, the α-SMA expression level of CAF-GM-1000TGF-β1 and CAF-GM-5000TGF-β1 was much higher than that of CAF-GM-500TGF-β1. The findings clearly indicates that TGF-β1 was effective in CAF activation. However, there is no significant difference in α-SMA expression level between CAF-GM-1000TGF-β1 and CAF-GM-5000TGF-β1. There would be due to an upper limitation in the CAF activation. Therefore, more than 5000 μg/ml of TGF-β1 concentration was not used to evaluate in this study. It is interesting that the addition of free TGF-β1 solution did not enable CAF to activate although the amount of TGF-β1 is the same or higher than that of TGF-β1 released. It is highly possible to say that the TGF-β1 release "in" CAF aggregates had a positive effect on activating CAF. This is because that the TGF-β1 is closely and uniformly released and exposed to cells.

Fig. 9A shows the cancer invasion after co-cultured of cancer cells with CAF-GM, various CAF-GM-TGF-β1, and CAF-GM + fTGF-β1. There was a good correlation between the α-SMA expression level and cancer invasion rate (Fig. 9B). We have designed a novel cancer invasion model using CAF aggregates incorporating GM containing a p53 inhibitor. This model was a promising tool for evaluating the cancer invasion *in vitro*. However, the cancer invasion rate did not become higher with an increasing drug concentration. It is reported that on a high drug concentration, the cancer invasion rate was significantly higher than that on lower concentrations [31]. For further research of cancer invasion or metastasis,

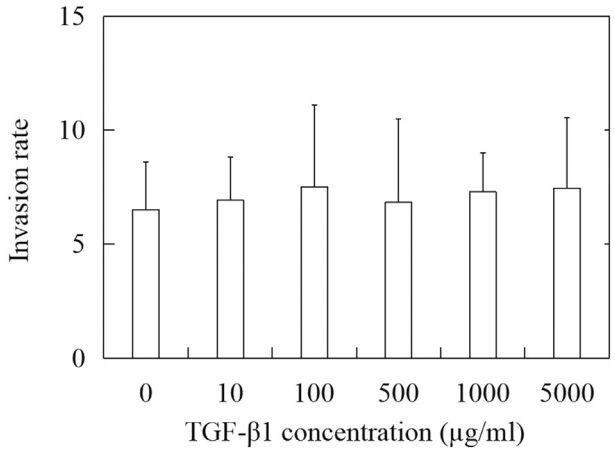

Fig. 12. Invasion rate of cancer cells by co-cultured with CAF-GM, CAF-GM by addition of 10, 100, 500, 1000, and 5000 μg/ml TGF-β1 solution.

cancer invasion model where invasion rate can be regulated should be developed. It is apparent from Fig. 9C this cancer invasion model of CAF aggregates incorporating GM-TGF-β1 can regulate the extent of the cancer invasion by simply changing the TGF-β1 concentration contained in GM. In addition, the MMP inhibitor treatment significantly decreased the invasion rate. Moreover, the secretion level of MMP-2 had an important role in the high cancer invasion rate (Fig. 11). Among the MMP, MMP-2 and 9 are essential to degrade the basement membrane. In this model, the secretion level of MMP-9 was not observed (data not shown). In this study, cancer cells would invade via the MMP-2 system *in vitro*. In the *in vivo* system, the cancer invasion via MMP is well known as a standard characterization (Fig. 1). Therefore, we designed a model to simulate the cancer invasion. By the addition of free TGF-β1, the cancer invasion rate did not change, irrespective of the TGF-β1 concentrations (Fig. 12). Again, this finding indicates the importance to release TGF-β1 in CAF aggregates for an efficient CAF activation and the consequent regulated tumor invasion phenomenon.

5. Conclusions

This model may be a useful tool to evaluate the difference in cancer invasion ability or therapeutic efficacy *in vitro*. As one experimental strategy to mimic the body environment, it would be important not only to achieve a 3D cell culture, but also to allow the growth factors to act on the cells. This study is the first report to design the cancer invasion model where the cancer invasion rate can be modified *in vitro* based on a combined 3D cell aggregates and growth factor release systems.

Declaration of Competing Interest

The authors declare no conflict of interest.

Acknowledgment

We would like to thank Assistant professor Jo for his kind support.

References

[1] Loizou GD. Animal-free chemical safety assessment. Front Pharmacol 2016;7:218.
[2] Mahler GJ, Esch MB, Stokol T, Hickman JJ, Shuler ML. Body-on-a-chip systems for animal-free toxicity testing. Altern Lab Anim 2016;44:469–78.
[3] Leist M, Hasiwa N, Rovida C, Daneshian M, Basketter D, Kimber I, et al. Consensus report on the future of animal-free systemic toxicity testing. ALTEX 2014;31:341–56.
[4] Pfuhler S, Fautz R, Ouedraogo G, Latil A, Kenny J, Moore C, et al. The Cosmetics Europe strategy for animal-free genotoxicity testing: project status up-date. Toxicol Vitro 2014;28:18–23.
[5] Mittal R, Woo FW, Castro CS, Cohen MA, Karanxha J, Mittal J, et al. Organ-on-chip models: implications in drug discovery and clinical applications. J Cell Physiol 2019;234:8352–80.
[6] Cochrane A, Albers HJ, Passier R, Mummery CL, van den Berg A, Orlova VV, et al. Advanced in vitro models of vascular biology: human induced pluripotent stem cells and organ-on-chip technology. Adv Drug Deliv Rev 2019;140:68–77.
[7] Zahedi-Tabar Z, Bagheri-Khoulenjani S, Mirzadeh H, Amanpour S. 3D in vitro cancerous tumor models: using 3D printers. Med Hypotheses 2019;124:91–4.
[8] Boutin ME, Kramer LL, Livi LL, Brown T, Moore C, Hoffman-Kim D. A three-dimensional neural spheroid model for capillary-like network formation. J Neurosci Methods 2018;299:55–63.
[9] Alexander Jr F, Eggert S, Wiest J. A novel lab-on-a-chip platform for spheroid metabolism monitoring. Cytotechnology 2018;70:375–86.
[10] Oyama H, Takahashi K, Tanaka Y, Takemoto H, Haga H. Long-term culture of human iPS cell-derived telencephalic neuron aggregates on collagen gel. Cell Struct Funct 2018;43:85–94.
[11] Nii T, Makino K, Tabata Y. Influence of shaking culture on the biological functions of cell aggregates incorporating gelatin hydrogel microspheres. J Biosci Bioeng 2019;128:606–12.
[12] Yu F, Hunziker W, Choudhury D. Engineering microfluidic organoid-on-a-chip platforms. Micromachines 2019;10.
[13] Nayak B, Balachander GM, Manjunath S, Rangarajan A, Chatterjee K. Tissue mimetic 3D scaffold for breast tumor-derived organoid culture toward personalized chemotherapy. Colloids Surf B Biointerfaces 2019;180:334–43.
[14] Kurosawa H. Methods for inducing embryoid body formation: in vitro differentiation system of embryonic stem cells. J Biosci Bioeng 2007;103:389–98.
[15] Fukuda J, Sakai Y, Nakazawa K. Novel hepatocyte culture system developed using microfabrication and collagen/polyethylene glycol microcontact printing. Biomaterials 2006;27:1061–70.
[16] Rodriguez-Enriquez S, Gallardo-Perez JC, Aviles-Salas A, Marin-Hernandez A, Carreno-Fuentes L, Maldonado-Lagunas V, et al. Energy metabolism transition in multi-cellular human tumor spheroids. J Cell Physiol 2008;216:189–97.
[17] Nelson LJ, Walker SW, Hayes PC, Plevris JN. Low-shear modelled microgravity environment maintains morphology and differentiated functionality of primary porcine hepatocyte cultures. Cells Tissues Organs 2010;192:125–40.
[18] Lin RZ, Chang HY. Recent advances in three-dimensional multicellular spheroid culture for biomedical research. Biotechnol J 2008;3:1172–84.
[19] Kellner K, Liebsch G, Klimant I, Wolfbeis OS, Blunk T, Schulz MB, et al. Determination of oxygen gradients in engineered tissue using a fluorescent sensor. Biotechnol Bioeng 2002;80:73–83.
[20] Compan V, Guzman J, Riande E. A potentiostatic study of oxygen transmissibility and permeability through hydrogel membranes. Biomaterials 1998;19:2139–45.
[21] Hayashi K, Tabata Y. Preparation of stem cell aggregates with gelatin microspheres to enhance biological functions. Acta Biomater 2011;7:2797–803.
[22] Kimura Y, Tabata Y. Controlled release of stromal-cell-derived factor-1 from gelatin hydrogels enhances angiogenesis. J Biomater Sci Polym 2010;21:37–51.
[23] Esaki J, Marui A, Tabata Y, Komeda M. Controlled release systems of angiogenic growth factors for cardiovascular diseases. Expet Opin Drug Deliv 2007;4:635–49.
[24] Tabata Y, Nagano A, Ikada Y. Biodegradation of hydrogel carrier incorporating fibroblast growth factor. Tissue Eng 1999;5:127–38.
[25] Ozeki M, Tabata Y. *In vivo* degradability of hydrogels prepared from different gelatins by various cross-linking methods. J Biomater Sci Polym 2005;16:549–61.
[26] Nitta N, Ohta S, Tanaka T, Takazakura R, Toyama T, Sonoda A, et al. An initial clinical study on the efficacy of cisplatin-releasing gelatin microspheres for metastatic liver tumors. Eur J Radiol 2009;71:519–26.
[27] Patel ZS, Yamamoto M, Ueda H, Tabata Y, Mikos AG. Biodegradable gelatin microparticles as delivery systems for the controlled release of bone morphogenetic protein-2. Acta Biomater 2008;4:1126–38.
[28] Ogawa T, Akazawa T, Tabata Y. In vitro proliferation and chondrogenic differentiation of rat bone marrow stem cells cultured with gelatin hydrogel microspheres for TGF-beta1 release. J Biomater Sci Polym Ed 2010;21:609–21.
[29] Kikuchi T, Kubota S, Asaumi K, Kawaki H, Nishida T, Kawata K, et al. Promotion of bone regeneration by CCN2 incorporated into gelatin hydrogel. Tissue Eng 2008;14:1089–98.
[30] Kushibiki T, Tomoshige R, Iwanaga K, Kakemi M, Tabata Y. Controlled release of plasmid DNA from hydrogels prepared from gelatin cationized by different amine compounds. J Contr Release 2006;112:249–56.
[31] Nii T, Makino K, Tabata Y. A cancer invasion model combined with cancer-associated fibroblasts aggregates incorporating gelatin hydrogel microspheres containing a p53 inhibitor. Tissue Eng C Methods 2019;25:711–20.
[32] Akagawa Y, Kubo T, Koretake K, Hayashi K, Doi K, Matsuura A, et al. Initial bone regeneration around fenestrated implants in Beagle dogs using basic

fibroblast growth factor-gelatin hydrogel complex with varying biodegradation rates. J Prosthodont Res 2009;53:41–7.
[33] Inoo K, Bando H, Tabata Y. Insulin secretion of mixed insulinoma aggregates-gelatin hydrogel microspheres after subcutaneous transplantation. Regen Ther 2018;8:38–45.
[34] Inoo K, Bando H, Tabata Y. Enhanced survival and insulin secretion of insulinoma cell aggregates by incorporating gelatin hydrogel microspheres. Regen Ther 2018;8:29–37.
[35] Tajima S, Tabata Y. Preparation of EpH4 and 3T3L1 cells aggregates incorporating gelatin hydrogel microspheres for a cell condition improvement. Regen Ther 2017;6:90–9.
[36] Tajima S, Tabata Y. Preparation of epithelial cell aggregates incorporating matrigel microspheres to enhance proliferation and differentiation of epithelial cells. Regen Ther 2017;7:34–44.
[37] Siegel RL, Miller KD, Jemal A. Cancer statistics, 2017. CA A Cancer J Clin 2017;67:7–30.
[38] Li H, Fan X, Houghton J. Tumor microenvironment: the role of the tumor stroma in cancer. J Cell Biochem 2007;101:805–15.
[39] Shan T, Chen S, Chen X, Lin WR, Li W, Ma J, et al. Cancer-associated fibroblasts enhance pancreatic cancer cell invasion by remodeling the metabolic conversion mechanism. Oncol Rep 2017;37:1971–9.
[40] Alvarez-Teijeiro S, Garcia-Inclan C, Villaronga MA, Casado P, Hermida-Prado F, Granda-Diaz R, et al. Factors secreted by cancer-associated fibroblasts that sustain cancer stem properties in head and neck squamous carcinoma cells as potential therapeutic targets. Cancers 2018;10.
[41] Shiga K, Hara M, Nagasaki T, Sato T, Takahashi H, Takeyama H. Cancer-associated fibroblasts: their characteristics and their roles in tumor growth. Cancers 2015;7:2443–58.
[42] Powell DW, Mifflin RC, Valentich JD, Crowe SE, Saada JI, West AB. Myofibroblasts. I. Paracrine cells important in health and disease. Am J Physiol 1999;277:C1–9.
[43] Infante JR, Matsubayashi H, Sato N, Tonascia J, Klein AP, Riall TA, et al. Peritumoral fibroblast SPARC expression and patient outcome with resectable pancreatic adenocarcinoma. J Clin Oncol 2007;25:319–25.
[44] Wandel E, Grasshoff A, Mittag M, Haustein UF, Saalbach A. Fibroblasts surrounding melanoma express elevated levels of matrix metalloproteinase-1 (MMP-1) and intercellular adhesion molecule-1 (ICAM-1) in vitro. Exp Dermatol 2000;9:34–41.
[45] Wilson CL, Heppner KJ, Labosky PA, Hogan BL, Matrisian LM. Intestinal tumorigenesis is suppressed in mice lacking the metalloproteinase matrilysin. Proc Natl Acad Sci U S A 1997;94:1402–7.
[46] Thomasset N, Lochter A, Sympson CJ, Lund LR, Williams DR, Behrendtsen O, et al. Expression of autoactivated stromelysin-1 in mammary glands of transgenic mice leads to a reactive stroma during early development. Am J Pathol 1998;153:457–67.
[47] Place AE, Jin Huh S, Polyak K. The microenvironment in breast cancer progression: biology and implications for treatment. Breast Cancer Res 2011;13:227.
[48] Boire A, Covic L, Agarwal A, Jacques S, Sherifi S, Kuliopulos A. PAR1 is a matrix metalloprotease-1 receptor that promotes invasion and tumorigenesis of breast cancer cells. Cell 2005;120:303–13.
[49] Takahashi M, Fukami S, Iwata N, Inoue K, Itohara S, Itoh H, et al. *In vivo* glioma growth requires host-derived matrix metalloproteinase 2 for maintenance of angioarchitecture. Pharmacol Res 2002;46:155–63.
[50] Kalluri R. The biology and function of fibroblasts in cancer. Nat Rev Canc 2016;16:582–98.
[51] Sandler RS, Halabi S, Baron JA, Budinger S, Paskett E, Keresztes R, et al. A randomized trial of aspirin to prevent colorectal adenomas in patients with previous colorectal cancer. N Engl J Med 2003;348:883–90.
[52] Tredan O, Galmarini CM, Patel K, Tannock IF. Drug resistance and the solid tumor microenvironment. J Natl Cancer Inst 2007;99:1441–54.
[53] Micke P, Ostman A. Tumour-stroma interaction: cancer-associated fibroblasts as novel targets in anti-cancer therapy? Lung Canc 2004;45(Suppl 2): S163–75.
[54] Casey TM, Eneman J, Crocker A, White J, Tessitore J, Stanley M, et al. Cancer associated fibroblasts stimulated by transforming growth factor beta1 (TGF-beta 1) increase invasion rate of tumor cells: a population study. Breast Canc Res Treat 2008;110:39–49.
[55] McEarchern JA, Kobie JJ, Mack V, Wu RS, Meade-Tollin L, Arteaga CL, et al. Invasion and metastasis of a mammary tumor involves TGF-beta signaling. Int J Canc 2001;91:76–82.
[56] Wick W, Platten M, Weller M. Glioma cell invasion: regulation of metalloproteinase activity by TGF-beta. J Neuro Oncol 2001;53:177–85.
[57] Tabata Y, Ikada Y. Synthesis of gelatin microspheres containing interferon. Pharm Res (N Y) 1989;6:422–7.
[58] Bratt-Leal AM, Carpenedo RL, Ungrin MD, Zandstra PW, McDevitt TC. Incorporation of biomaterials in multicellular aggregates modulates pluripotent stem cell differentiation. Biomaterials 2011;32:48–56.
[59] Cheng CY, Pho QH, Wu XY, Chin TY, Chen CM, Fang PH, et al. PLGA microspheres loaded with beta-cyclodextrin complexes of epigallocatechin-3-gallate for the anti-inflammatory properties in activated microglial cells. Polymers 2018;10.
[60] Alenezi A, Naito Y, Terukina T, Prananingrum W, Jinno Y, Tagami T, et al. Controlled release of clarithromycin from PLGA microspheres enhances bone regeneration in rabbit calvaria defects. J Biomed Mater Res B Appl Biomater 2018;106:201–8.
[61] Yuan Y, Shi X, Gan Z, Wang F. Modification of porous PLGA microspheres by poly-l-lysine for use as tissue engineering scaffolds. Colloids Surf B Biointerfaces 2018;161:162–8.
[62] Nii T, Takeuchi I, Kimura Y, Makino K. Effects of the conformation of PLGA molecules in the organic solvent on the aerodynamic diameter of spray dried microparticles. Colloids Surf, A 2018;539:347–53.
[63] Thaya R, Vaseeharan B, Sivakamavalli J, Iswarya A, Govindarajan M, Alharbi NS, et al. Synthesis of chitosan-alginate microspheres with high antimicrobial and antibiofilm activity against multi-drug resistant microbial pathogens. Microb Pathog 2018;114:17–24.
[64] Zeng J, Li L, Zhang H, Li J, Liu L, Zhou G, et al. Radiopaque and uniform alginate microspheres loaded with tantalum nanoparticles for real-time imaging during transcatheter arterial embolization. Theranostics 2018;8: 4591–600.
[65] Zekorn D. Intravascular retention, dispersal, excretion and break-down of gelatin plasma substitutes. Bibl Haematol 1969;33:131–40.
[66] Narita A, Takahara M, Ogino T, Fukushima S, Kimura Y, Tabata Y. Effect of gelatin hydrogel incorporating fibroblast growth factor 2 on human meniscal cells in an organ culture model. Knee 2009;16:285–9.
[67] Takahashi Y, Yamamoto M, Tabata Y. Osteogenic differentiation of mesenchymal stem cells in biodegradable sponges composed of gelatin and beta-tricalcium phosphate. Biomaterials 2005;26:3587–96.
[68] Tajima S, Tabata Y. Preparation and functional evaluation of cell aggregates incorporating gelatin microspheres with different degradabilities. J Tissue Eng Regen Med 2013;7:801–11.
[69] Sappino AP, Skalli O, Jackson B, Schurch W, Gabbiani G. Smooth-muscle differentiation in stromal cells of malignant and non-malignant breast tissues. Int J Canc 1988;41:707–12.
[70] Orimo A, Weinberg RA. Heterogeneity of stromal fibroblasts in tumors. Canc Biol Ther 2007;6:618–9.